

PACS numbers: 61.46.Hk, 62.23.St

ZINC OXIDE NANOSTRUCTURES BY OXIDATION OF ZINC FILMS DEPOSITED ON OXIDIZED SILICON SUBSTRATE

H.J. Pandya¹, S. Chandra²

¹ Instrument Design and Development Centre,
Indian Institute of Technology Delhi,
Hauz Khas, New Delhi, 110016, India
E-mail: hjpele@yahoo.com

² Centre for Applied Research in Electronics,
Indian Institute of Technology Delhi,
Hauz Khas, New Delhi, 110016, India

In this work, we report the preparation and characterization of nanostructured ZnO film prepared by a novel technique of oxidation of zinc film. Zinc thin films of thicknesses 100, 200 and 500 nm were deposited on oxidized Si wafer by thermal evaporation technique. The as-deposited films were then annealed in a furnace for 6 hours under normal atmospheric condition. The annealing was carried out in the temperature range 100-500 °C. Electron microscopic studies indicated that the film of 100 nm thickness consisted of hexagonal nanodisks while the 200 nm film resulted in stack of nano hexagonal disks of ZnO after annealing. On the other hand, the 500 nm film contained mixture of nanoflakes and nanowires of ZnO following annealing. The growth of ZnO nanostructures depends on annealing temperature and the Zn film thickness. The nanostructures of ZnO can be grown on large area (2 inch oxidized silicon wafer in present case) thus making it feasible to use these for device fabrication such as gas sensors. The X-ray diffractogram (XRD) study has been carried out to investigate the crystal structure. Possible mechanism is proposed to explain the growth of these ZnO nanostructures.

Keywords: ZINC, THIN FILMS, ZINC OXIDE, SYNTHESIS, NANOSTRUCTURES.

(Received 04 February 2011)

1. INTRODUCTION

Recently, the semiconducting nanostructures such as nanowires, nanorods, nanotubes, and nanobelts have caught considerable attention due to their potential application in diverse fields such as electronics, optoelectronics, and sensor devices [1]. The devices fabricated from the nanostructures are expected to have a unique and interesting quality due to quantum confinement effect and dimensionality. Zinc oxide (ZnO) is a wide band gap semiconductor, which is an excellent candidate for use in semiconducting, photoconducting, piezoelectric and optical waveguide materials [2-4]. It has a hexagonal close-packed structure (wurtzite type) with a band gap of 3.37 eV, and a large exciton binding energy of 60 meV [2]. It also exhibits excellent piezoelectric, chemical, and optical properties for various applications such as ultraviolet-blue emission devices, piezoelectric devices, and vapor gas sensor devices [5]. ZnO nanostructure can be synthesized by various techniques such as chemical vapor deposition (CVD) [6], pulsed laser

deposition (PLD) [7], metalorganic vapor phase epitaxy (MOVPE) [8], molecular beam epitaxy (MBE) [9], electrochemical deposition [10], thermal evaporation [11, 12] and sputtering [13,14].

In the present work, we report synthesis of ZnO nanostructures by oxidation of zinc thin films without using a catalyst. The ZnO nanostructures were grown on large area (2 inch diameter oxidized silicon wafer) thus making it feasible to use these for device fabrication such as gas sensors.

2. EXPERIMENTAL WORK

Zinc films were deposited using thermal evaporation. The silicon substrates were cleaned by standard cleaning procedures and SiO₂ (1 μm) was grown by thermal oxidation process. The zinc deposition was carried out without any external substrate heating. The thickness of the zinc film was kept to be 100 nm, 200 nm and 500 nm. As-deposited zinc films of 100 nm, 200 nm and 500 nm were placed in a ceramic boat and heated to 100 °C, 200 °C and 500 °C respectively in air for 6 hours in a box furnace. Before unloading the annealed films from the furnace, these were allowed to cool down to room temperature. It was observed that, following the annealing process, the color of the films turns white from the gray color of zinc films. XRD measurements of the annealed films were performed on Philips X-ray diffractometer (Model: XPert) and diffracted intensities were collected in $\theta-2\theta$ scan mode. Scanning electron microscope (Zeiss, EVO 50) was used for observing the surface morphology of the annealed films.

3. RESULT AND DISCUSSION

To know the crystallographic orientation of the annealed films, the XRD patterns were obtained. These are shown in Fig. 1. It was found that the annealed film was ZnO with hexagonal wurtzite structure (JCPDS 36-1451). In addition, the intensity of diffraction peaks from Zn was found weaker as thickness and annealing temperature increased.

Surface morphology of ZnO film obtained by annealing of 100 nm Zn film at 100 °C for 6 hours is shown in Fig. 2 a. The SEM picture of the corresponding Zn film before annealing is shown in Fig. 2 b. Randomly placed hexagonal disk-like structures having a perfect hexagonal geometry were observed for ZnO. The hexagonal blocks had size ranging from 200 nm to 600 nm. As mentioned earlier, no catalyst was used in the growth of the ZnO nano hexagonal blocks in this study. Accordingly, the vapor-liquid-solid (VLS) mechanism cannot be responsible for their growth. The following mechanism is proposed for the growth of hexagonal discs. For the 100 nm Zn film, the SEM picture shows nano-sized discrete particles evenly spread over the continuous Zn film. On annealing at 100 °C for 6 h in air, these Zn nanostructures grow in size forming ZnO hexagonal blocks ranging in size from 200-600 nm.

The increase in hexagonal size is presumably due to growth of ZnO from much smaller nuclei of Zn present in the original film [15-16]. It is further presumed that the Zn material present as continuous film is almost fully consumed in this process to give comparatively large sized hexagonal structures of ZnO. This hypothesis is supported by a very weak peak of Zn observed in the XRD of the annealed film, which primarily shows peaks corresponding to ZnO only.

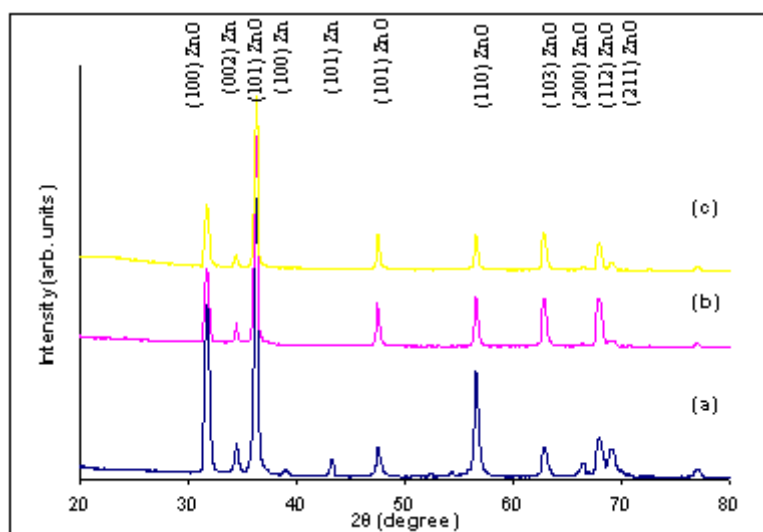


Fig. 1 – XRD results of ZnO film (a) 100 nm Zn film after annealing at 100 °C, (b) 200 nm Zn film after annealing at 200 °C and (c) 500 nm Zn film after annealing at 500 °C. The annealing time is 6 hours for all the samples

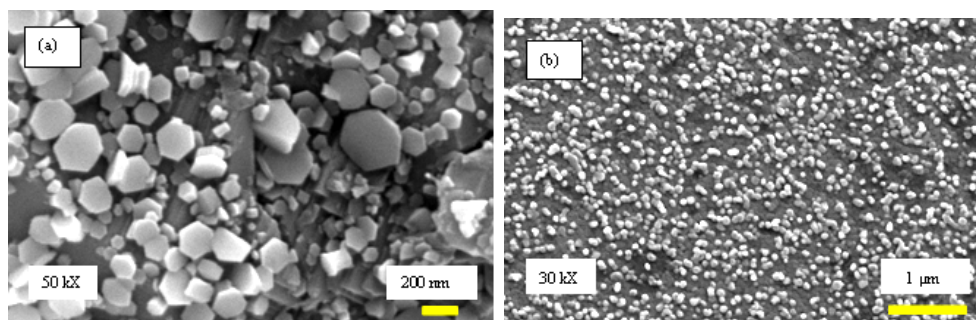


Fig. 2 – SEM image of (a) ZnO film after annealing Zn film (100 nm thick) at 100 °C for 6 h, (b) as-deposited Zn film (100 nm thick).

Fig. 3 a and Fig. 3 b respectively shows surface morphology of the ZnO film obtained by annealing at 200 °C for 6 hours and the corresponding as-deposited Zn film having 200 nm thickness. From Fig. 3 a, it can be inferred that annealing results in the stacks of well defined nanodisks grown perpendicular to the growth axis but otherwise randomly arranged. From the XRD pattern of Fig. 1 b, it can be observed that all diffraction peaks match with the wurtzite structural ZnO. The strong diffraction peaks appear at 31.8° and 36.5°, which correspond to 100 and 101 planes of wurtzite ZnO. It is further observed that the peak corresponding to Zn is now almost absent in the XRD. This implies that complete conversion of Zn into ZnO has been accomplished. The mechanism responsible for the growth of stack of ZnO nanodisks is not fully understood.

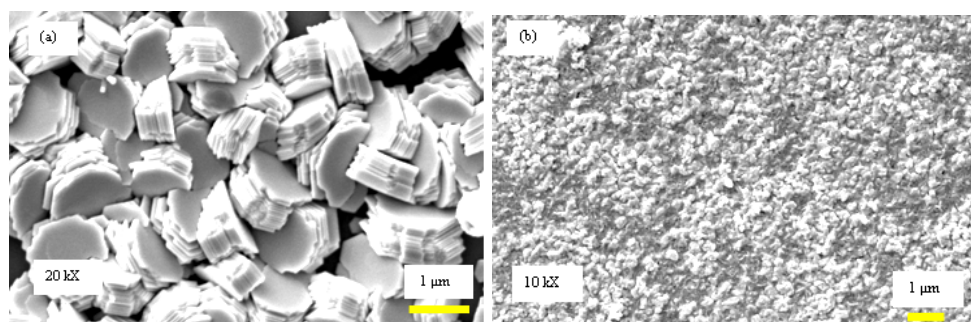


Fig. 3 – SEM image of (a) ZnO film after annealing Zn film (200 nm thick) at 200 °C for 6 h, (b) as-deposited Zn film (200 nm thick)

Fig. 4 a and b respectively shows surface morphology of the ZnO film obtained by annealing at 500 °C for 6 hours and the corresponding as-deposited Zn film having 500 nm thickness. The Zn film (500 nm) annealed at 500 °C for six hours resulted in growth of microflakes with small percentage of nanowires. The microflakes and nanowires were randomly orientated with respect to the surface of the oxidized silicon substrate. The diameters of the ZnO nanowires were between 100 and 150 nm, and the size of the microflakes was in the range of 1-4 μm. The XRD spectra of highly oriented thin film of ZnO has a predominant (002) reflection [17]. In contrast, Fig. 1 c shows that the (0 0 2) reflection is weaker than the (100), (101) and (110) reflections. As reported elsewhere [17-18], the weaker (002) reflection indicates that the ZnO microflakes and nanowires were polycrystalline. This image provides evidence of oriented attachment growth, and that the ZnO microflakes matrix was composed of many nanoparticles attached side-by-side. A similar phenomenon was also observed by other workers in undoped ZnO nanorods, hollow micro-hemispheres [19] and co-doped ZnO nanosheets-based structures [20].

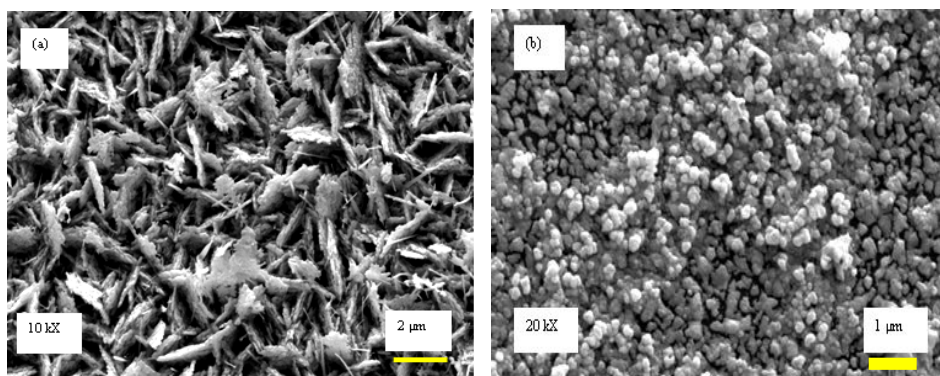


Fig. 4 – SEM image of (a) ZnO film after annealing Zn film (500 nm thick) at 500 °C for 6 h, (b) as-deposited Zn film (500 nm thick)

When the annealing temperature for 500 nm film was decreased to 300 °C, ZnO nanoparticles having a uniform size were observed, as shown in Fig. 5. This shows that the higher temperature of annealing (500 °C) favors the formation of the microflakes with small percentage of nanowires.

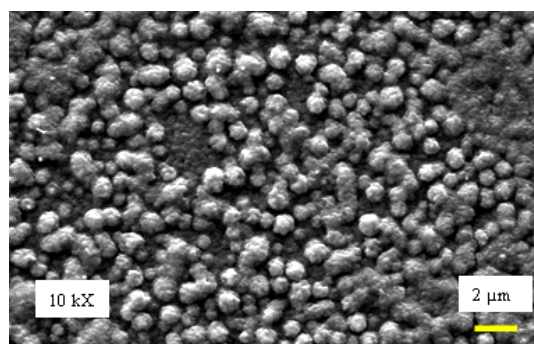


Fig. 5 – SEM image of ZnO film after annealing Zn film (500 nm thick film) at 300 °C for 6 h

4. CONCLUSIONS

In summary, we have demonstrated a simple and convenient route for synthesis of ZnO nanostructures on oxidized silicon wafers without using any catalyst. In particular, zinc film of 200 nm thickness and annealed at 200 °C for 6 h. results in well defined stack of hexagonal nanodisks. The type of growth of ZnO nanostructures strongly depends on thickness of zinc film, annealing temperature and time. These nanostructures can be used as a class of ZnO semiconducting nanostructures for device fabrication.

REFERENCES

1. X. Duan, C.M. Lieber, *Adv. Mater.* **12**, 298 (2000).
2. S.J. Pearton, D.P. Norton, K. Ip, et al., *Prog. Mater. Sci.* **50**, 293 (2005).
3. D.C. Look, *Mater. Sci. Eng. B* **80**, 383 (2001).
4. S. Choopun, R.D. Vispute, W. Noch, et al., *Appl. Phys. Lett.* **75**, 3947 (1999).
5. Q. Wan, H. Li, Y.J. Chen, T.H. Wang, et al., *Appl. Phys. Lett.* **84**, 3654 (2004).
6. M. Saitoh, N. Tanaka, Y. Ueda, et al., *Jpn. J. Appl. Phys.* **38**, L586 (1999).
7. S. Choopun, H. Tabata, T. Kawai, *J. Crystal Growth* **274**, 167 (2005).
8. W.I. Park, D.H. Kim, S.-W. Jung, G.-C. Yi, *Appl. Phys. Lett.* **80**, 4232 (2002).
9. Y.W. Heo, V. Varadarajan, M. Kaufman, et al., *Appl. Phys. Lett.* **81**, 3046 (2002).
10. M.J. Zheng, L.D. Zhang, G.H. Li, W.Z. Shen, *Chem. Phys. Lett.* **363**, 123 (2002).
11. J.Q. Hu, X.L. Ma, Z.Y. Xie, N.B. Wong, C.S. Lee, S.T. Lee, *Chem. Phys. Lett.* **344**, 97 (2001).
12. B.D. Yao, Y.F. Chan, N. Wang, *Appl. Phys. Lett.* **81**, 757 (2002).
13. Y.S. Chang, J.M. Ting, *Thin Solid Films* **398–399**, 29 (2001).
14. W.T. Chiou, W.Y. Wu, J.M. Ting, *Diamond Related Mater.* **12**, 1841 (2003).
15. X. Hong, D. Wang, G.R. Li, C.Y. Su, D.B. Kuang, Y.X. Tong, *J. Phys. Chem. C* **113**, 13574 (2009).
16. C.X. Xu, X.W. Sun, Z.L. Dong, M.B. Yu, *Appl. Phys. Lett.* **85**, 3878 (2004).
17. X.T. Zhang, Y.C. Liu, L.G. Zhang, et al., *Appl. Phys. Lett.* **92**, 3293 (2002).
18. G. Sberveglieri, S. Gropelli, P. Nelli, A. Tintinelli, G. Giunta, *Sens. Actuators B* **25**, 588 (1995).
19. M. Mo, J.C. Yu, Z.L. Zhang, S.K. Li, *Adv. Mater.* **17**, 756 (2005).
20. X.F. Wang, J.B. Xu, N. Ke, J.G. Yu, J. Wang, Q. Li, R. Zhang, *Appl. Phys. Lett.* **88**, 223108 (2006).